Review of Scientific Instruments

Measurement performance assessment for the ITER CXRS Edge diagnostic system

Cite as: Rev. Sci. Instrum. **92**, 053517 (2021); https://doi.org/10.1063/5.0042029
Submitted: 28 December 2020 • Accepted: 21 April 2021 • Published Online: 07 May 2021

S. V. Serov, M. De Bock, M. G. von Hellermann, et al.

Review of Scientific Instruments ARTICLE scitation.org/journal/rsi

Measurement performance assessment for the ITER CXRS Edge diagnostic system

Cite as: Rev. Sci. Instrum. 92, 053517 (2021); doi: 10.1063/5.0042029
Submitted: 28 December 2020 • Accepted: 21 April 2021 •
Published Online: 7 May 2021

S. V. Serov,[1,a)] M. De Bock,[2] M. G. von Hellermann,[3] and S. N. Tugarinov[1]

AFFILIATIONS

[1] Institution "Project Center ITER", 123182 Moscow, Russia
[2] ITER Organization, Route de Vinon-sur-Verdon, CS 90 046, 13067 St. Paul Lez Durance Cedex, France
[3] Institute for Energy and Climate Research IEK-4, Forschungszentrum Jülich GmbH, 52425 Jülich, Germany

Note: Paper published as part of the Special Topic on Proceedings of the 23rd Topical Conference on High-Temperature Plasma Diagnostics.
[a)] **Author to whom correspondence should be addressed:** s.serov@iterrf.ru

ABSTRACT

Measurement performance assessment has been carried out for the latest design of the ITER Charge Exchange Recombination Spectroscopy (CXRS) Edge diagnostic system. Several plasma scenarios, covering all expected baseline operation regimes for ITER, were used. Various impurity (He, Be, C, and Ne) concentrations for the system whole spatial range ($0.5 < r/a < 1.0$) were considered. Statistical errors for the measurements of low-Z impurity temperature, density, and rotation velocity were calculated. Other non-statistical error sources were reviewed, including the presence of wall reflections, effects on the active charge-exchange line shape, calibration, and positioning uncertainties. Minimal impurity concentrations, allowing measurements with required accuracy, were obtained. It was shown that the CXRS Edge system will be able to measure primary plasma parameters with required accuracy, space, and time resolution.

I. INTRODUCTION

Charge eXchange Recombination Spectroscopy (CXRS) is a powerful diagnostic tool for ion temperature, low-Z impurity density, and plasma rotation velocity measurements in fusion devices.[1,2] These plasma parameters are extracted from the active charge-exchange (CX) spectral line, emitted during high-energy neutral beam injection into plasma. The measurements could become complicated because of the low signal-to-noise ratio (SNR) and the presence of the other spectral lines due to CX reactions with the edge neutrals[3] (passive CX line) and due to the electron impact excitation[4] (edge lines). Therefore, measurement performance assessment is important for the development of the CXRS diagnostic.

First feasibility studies for ITER[5] showed that local measurements of light impurity densities, ion temperatures, and rotation profiles will be possible only outside of $r/a = 0.5$ with a 0.1 s time resolution for the highest density plasmas considered. In Refs. 6–8, it was shown that optimized viewing geometry and spectroscopic equipment will allow increasing the SNR significantly. The feasibility of CXRS measurements was demonstrated up to $r/a = 0.3$ for the highest plasma density $n_e = 1.4 \times 10^{20}$ m^{-3}.

Further development for the CXRS diagnostic for ITER, including design optimization and modeling, is described in Refs. 9–14. With the aim of providing optimum radial resolution as well as the means for complementary toroidal and poloidal velocity measurements, three observation periscopes have been designed: CXRS Core[15] ($0 \leqslant r/a \leqslant 0,6$), CXRS Edge[16] ($0,5 \leqslant r/a \leqslant 1$), and CXRS Pedestal ($0,85 \leqslant r/a \leqslant 1$). Figure 1 shows the present layout for the ITER CXRS diagnostic lines of sight (LOS): CXRS Edge and Pedestal are mostly toroidal systems with a $\pm 10^{\circ}$ angle to the horizontal plane, while for the Core system, this angle is about 55°.

This paper describes modeling, carried out for the latest CXRS Edge system design. Several scenarios, covering all expected baseline operation regimes for ITER, were used. The modeling was done for various low-Z impurity (He, Be, C, and Ne) concentrations for the system whole spatial range ($0.5 < r/a < 1.0$). Statistical errors for ion temperature, density, and rotation velocity were calculated. Minimal concentrations, allowing measurements with the required accuracy, were obtained. Effort was made to review other non-statistical error sources for the CXRS measurements, including wall reflections, multiple tungsten lines in CX spectra, effects on the active CX line

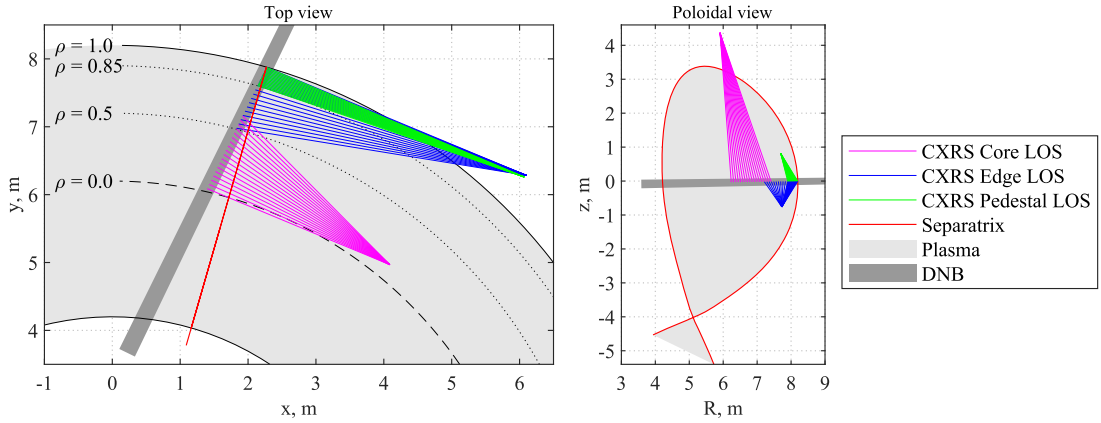

FIG. 1. The layout of the CXRS Core, CXRS Edge, and CXRS Pedestal lines of sight (LOS) looking at the diagnostic neutral beam (DNB). Various plasma radii ($\rho = r/a$) and the top view of the separatrix are indicated on the left image. The right image shows the plasma poloidal cross section.

shape, calibration, and positioning uncertainties. Consideration of the major error sources showed that the CXRS Edge system will be able to meet all ITER measurement requirements, apart from the requirements for the poloidal rotation velocity measurements.

II. CXRS SPECTRA MODELING

To assess the CXRS Edge measurement performance, the Simulation of Spectra (SOS) code[17] has been utilized. It was developed for predicting beam-induced spectroscopy diagnostic performance on fusion devices. In particular, it has models for all main CXRS spectrum components and could also be used for spectra fitting and error estimation. The spectrum is constructed from the following components, modeled separately: active CX line, passive CX line, edge electron impact excitation lines, bremsstrahlung continuum, and statistical noise. The obtained spectrum is fitted using least-squares minimization procedure. Intensity, temperature, and rotation velocity errors are calculated from the active CX line fitting 95% confidence intervals (corresponding to $\pm 2\sigma$). The main source of atomic data is the ADAS database.[18]

The SOS models were validated using experimental data from several tokamaks, e.g., JET,[19] TEXTOR,[20] and EAST.[21] The benchmarking process will not be discussed in this paper. Results of the benchmarking against JET experimental data[16] demonstrate that the SOS code allows reasonable CXRS spectra predictions and could be used for active spectroscopy diagnostic development for ITER. However, there is a need for more detailed and careful benchmarking, which is currently ongoing.

According to the ITER requirements,[22] CXRS diagnostics should measure ion temperature radial profiles, impurity density profiles, and rotation velocity profiles with a 100 ms time resolution and a 10%–30% accuracy. The spatial resolution should be 20 mm for the plasma boundary ($r/a > 0.85$) and 66 mm for the center part of the plasma column ($0, 0 \leqslant r/a \leqslant 0.85$). Table I shows the extraction from the ITER Project Requirements and lists all primary measurement parameters assigned to the CXRS diagnostics.

Figure 2 shows electron density, electron temperature, ion temperature, and rotation velocity radial profiles for the scenarios used for the modeling. Several inductive, steady-state, and hybrid scenarios were considered. More details on integrated modeling for different operational scenarios could be found in Ref. 23. Modeling was carried out for the whole spatial range ($0.5 < r/a < 1.0$) of the CXRS Edge system for He Be, C, and Ne. For these elements, CX-induced lines are covered by the three channels of high resolution, High Etendue Spectrometer (HES),[24] based on transmission holographic diffraction gratings. Be IV (6–5) 4658 Å and He II (4–3) 4686 Å lines are in the so called "blue" channel; Ne X (11–10) 5249 Å and C VI (8–7) 5291 Å lines are in the "green" channel; and H-alpha (3–2) 6563 Å and beam emission H-alpha lines are in the "red" channel.

Various concentrations of He Be, C, and Ne were examined, going down from reference values, expected for ITER: $n_{He} = 0.04n_e$, $n_{Be} = 0.02n_e$, $n_C = 0.001n_e$, and $n_{Ne} = 0.003n_e$. Impurities were assumed to have the same radial profile shape as n_e. The same ion temperature profile was used for hydrogen and all impurities. The following DNB parameters are used: $E = 100$ keV, FWHM size $\approx 0.2 \times 0.2$ m^2, and power: 1.4 MW. A light collection system transmission of 5% was used. The spectrometer dispersion was 3.4, 3.6, and 5.0 A/mm for the "blue," "green," and "red" channels, respectively. The integration time was 100 ms for a detector with a 10 μm pixel size and a sensor resolution of 2048 × 2048 pixels.

TABLE I. Measurement parameters with the corresponding requirements assigned to the CXRS Edge diagnostic system.

Measurement parameter	Condition	Range	Spatial resolution	Accuracy (%)
v_{pol}	⋯	1–50 km/s	$a/30$	30
v_{tor}	⋯	1–200 km/s	$a/30$	30
Z_{eff} profile	⋯	1.0–5.0	$a/10$	10
Core T_i	$r/a < 0.85$	0.5–40 keV	$a/30$	10
Edge T_i	$r/a > 0.85$	0.05–10 keV	$a/100$	10
Core n_{He}/n_e	$r/a < 0.85$	1%–20%	$a/10$	10
n_{He^3} profile	$r/a < 0.85$	1%–10%	$a/10$	10
$n_{Z\leqslant 10}$ profile	⋯	0.005–0.2 n_e	$a/10$	20

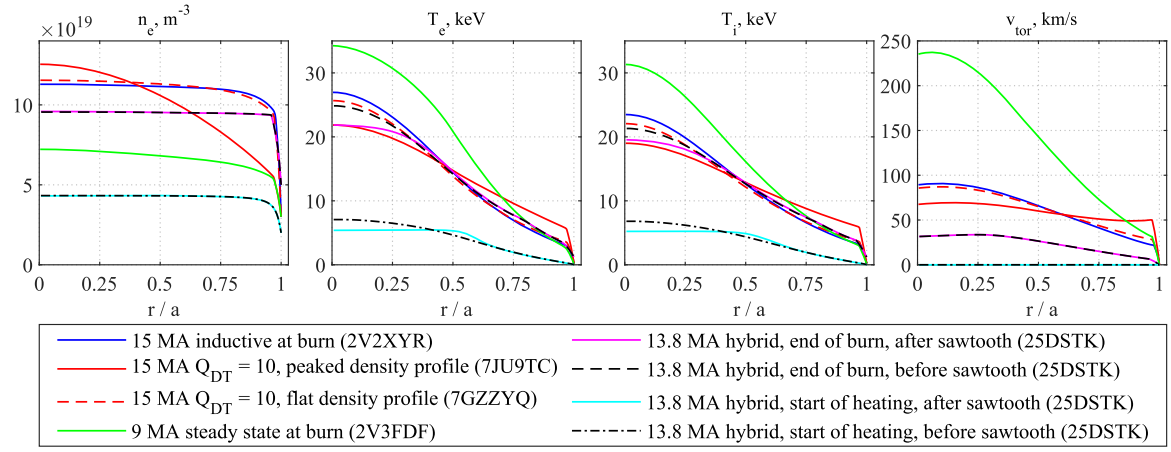

FIG. 2. n_e, T_e, T_i, and v_{tor} radial profiles for ITER operation scenarios used for the modeling. The ITER document reference for each scenario is indicated.

III. MODELING RESULTS

The main outcome of the simulation is a spectral profile, which is fitted to calculate statistical errors for the measurements of the light impurity concentration, ion temperature, and projection of the plasma rotation velocity on the LOS direction (observed velocity). An example of modeled spectra for He and Be is shown in Fig. 3. As one would expect, the largest values for the concentration and temperature errors were found for the 15 MA inductive scenario with the highest density for the outer plasma. Relative errors for the observed rotation velocity had the largest value for the 13.8 MA hybrid scenario at the end of burn after sawtooth. For the scenarios without the plasma rotation, absolute errors were calculated for the observed velocity.

Impurity concentration measurement errors are illustrated by the top row images in Fig. 4. Two-dimensional plots indicate the dependence on the concentration (shown along the horizontal axis) and observation points, that is, minor plasma radii (shown along the vertical axis). The yellow area corresponds to the error values exceeding those in the ITER requirements from Table I, and red vertical lines indicate minimal concentration values from the table. Blue vertical lines indicate the reference concentrations used for the modeling. The bottom row images in Fig. 4 illustrate the errors for the ion temperature measurements using He, Be, C, and Ne active CX lines.

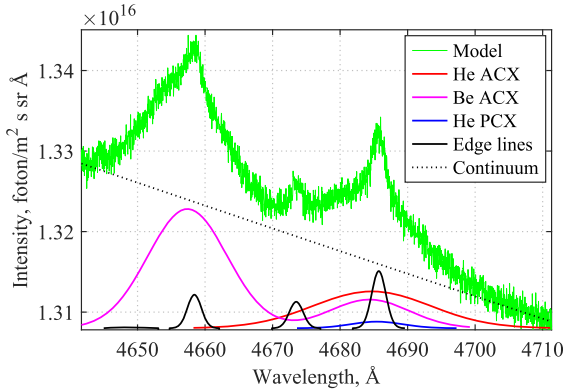

FIG. 3. Modeled "blue" channel CXRS spectrum with fitting for the 15 MA inductive scenario at r/a = 0.5. It includes three active CX lines: Be IV (6–5) 4658 Å, Be IV (8–6) 4685 Å, and He II (4–3) 4686 Å.

The error increase toward the plasma core can be accounted for by the significant attenuation of the DNB. Contours on each image have a leap between $r/a = 0.85$ and $r/a = 0.9$ because the CXRS Edge central views ($r/a \leqslant 0.85$) will use spectrometers with a wider entrance slit (1 mm). It is essential to collect more light in order to improve the SNR for the weak active CX signal from the central plasma.

Figure 5 illustrates statistical errors for the LOS projection of the rotation velocity. Top row images show relative statistical errors (in percentage) for the 13.8 MA hybrid scenario at the end of burn after sawtooth. It could be noted that relative velocity errors increase not only in the plasma center but also at the plasma edge due to the small magnitude of the rotation velocity. Bottom row images show absolute errors for the 13.8 MA hybrid scenario at the start of heating after sawtooth. The green area marks absolute errors below 0.3 km/s. This value is obtained from Table I by multiplying a minimal measurable velocity of 1 km/s and 30% accuracy.

Data from Figs. 4 and 5 have been used to determine minimal impurity concentrations, allowing measurements with the needed accuracy for the whole spatial range of the CXRS Edge system. These concentrations are summarized in Table II, where the reference concentrations and minimal concentrations from the requirements (Table I) are also indicated. It could be seen that regarding statistical errors, the CXRS Edge system design will allow plasma parameter profile measurements according to the ITER requirements. Light impurity concentrations could be measured with a good margin, except for He. For the ion temperature measurements, He, Be, and Ne lines could be used. For scenarios with $v_{rot}(r/a = 0,5)$ greater than ~10 km/s, the LOS projection of the rotation velocity could be measured using all active CX lines, with the smallest errors expected for Ne. For the scenarios with negligible rotation velocity, most accurate measurements would again be possible using the Ne line.

Apart from the considered statistical errors, other (non-statistical) errors should be taken into account. Here, we will only briefly go through various factors that could reduce measurement

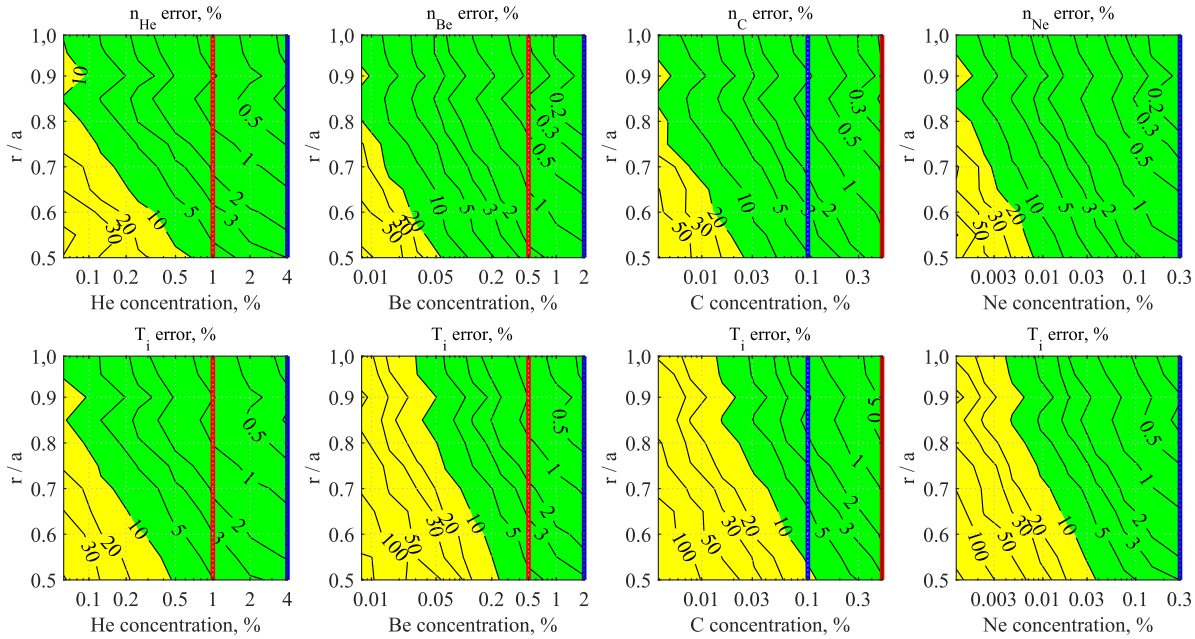

FIG. 4. n_Z (top row) and T_i (bottom row) relative errors (in percentage) for the 15 MA inductive scenario depending on the impurity concentrations. Yellow areas correspond to the errors exceeding those in the ITER requirements, and vertical red lines indicate minimal concentration requirements. Vertical blue lines indicate the reference concentrations.

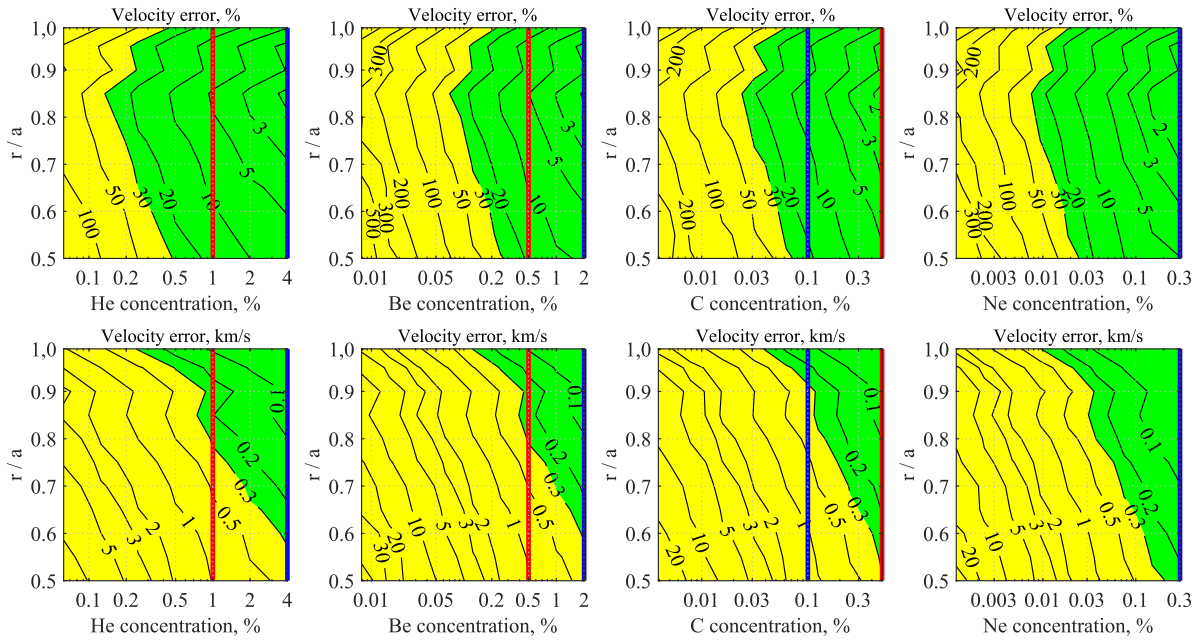

FIG. 5. Relative errors (in %) of the observed rotation velocity for the 13.8 MA hybrid scenario at the end of burn after sawtooth (top row) and absolute velocity errors for the 13.8 MA hybrid scenario at the start of heating after sawtooth (bottom row) depending on the impurity concentrations. Yellow areas correspond to the errors exceeding those in the ITER requirements, and vertical red lines indicate minimal concentration requirements. Vertical blue lines indicate the reference concentrations.

TABLE II. Minimal impurity concentrations, allowing measurements with the required accuracy. Reference concentrations and minimal concentrations from the requirements are also indicated.

Measured parameter	Accuracy requirement	Minimal concentrations (%)			
		n_{He}	n_{Be}	n_C	n_{Ne}
n_z (n_{He})	20% (10%)	0.7	0.06	0.03	0.008
T_i	10%	0.5	0.25	0.15	0.04
v (for $v > 0$)	30%	0.5	0.3	0.07	0.03
v (for $v \sim 0$)	0.3 km/s	>4	>2	0.5	0.2
Reference concentration		4.0	2.0	0.1	0.3
Concentration from the requirements		1.0	0.5	0.5	0.5

accuracy. The detailed review of all possible sources of uncertainties goes beyond the scope of this paper.

Reflected light from the metallic first wall becomes a big complication for all spectroscopic diagnostics on ITER. However, the only notable effect for the CXRS turns out to be a $\sqrt{2}$ increase in errors due to the continuum level rise.[25] Another complicating factor is the emission of multiple tungsten lines, appearing in the CXRS spectra. That problem could be dealt with by a clear identification of each W line.[26]

Atomic physics effects could have a significant influence on the CX line shape. Zeeman and Fine structure broadening are not considered is the SOS code but could be routinely taken into account.[27] SOS modeling of the Halo effect showed that it could lead up to 20% boost for the active CX line intensity, without changing line shape significantly.[17] Models for the plume effect indicate that it could introduce errors up to 40% to the CX line intensity.[17,28] The CX cross-sectional effect could also introduce significant errors (up to 50 km/s) in rotation velocity measurements.[17] Therefore, these effects definitely need to be modeled and taken into account when processing ITER CXRS spectra.

Geometrical limitations for the positions of the CXRS Edge and CXRS Pedestal periscopes lead to a small angle between LOS of these systems in the vertical plane. This introduces significant errors when calculating the plasma poloidal rotation velocity from the measured projections of the rotation on the CXRS Edge and CXRS Pedestal LOS directions. The error for v_{pol} is estimated to be 2.5 km/s. Keeping in mind another factor, spectrometer wavelength calibration, which could lead to errors of the same magnitude,[29] the accuracy for the plasma poloidal rotation velocity measurements using both edge and pedestal periscopes is estimated to be 5 km/s.

IV. SUMMARY AND FUTURE WORK

Measurement performance assessment for the ITER CXRS Edge diagnostic system was carried out using the SOS code. Various scenarios and different impurity concentrations were considered. It was shown that concentrations could be measured with required accuracy, given the reliable modeling of the effects on the active CX line shape. For the ion temperature measurements, He, Be, and Ne lines could be used. Toroidal rotation velocity measurements would be most accurate for Ne. The most difficult will be the measurement of the poloidal rotation velocity: the possible accuracy should be about 5 km/s.

For the future work, quantitative benchmarking of the SOS code against various JET discharges is planned. Validation of the SOS models for the effects on the active CX line shape, crucial for the extraction of the plasma parameters, is also foreseen.

ACKNOWLEDGMENTS

This work was carried out in accordance with the state contract dated April 21, 2020 (Grant No. H.4a.241.19.20.1042).

The views and opinions expressed herein do not necessarily reflect those of the ITER Organization.

DATA AVAILABILITY

The data that support the findings of this study are available from the corresponding author upon reasonable request.

REFERENCES

[1] R. J. Fonck, D. S. Darrow, and K. P. Jaehnig, Phys. Rev. A **29**, 3288 (1984).
[2] R. C. Isler, Plasma Phys. Controlled Fusion **36**, 171 (1994).
[3] M. Tunklev *et al.*, Plasma Phys. Controlled Fusion **41**, 985 (1999).
[4] E. Viezzer, T. Pütterich, R. Dux, A. Kallenbach, and ASDEX Upgrade Team, Plasma Phys. Controlled Fusion **53**, 035002 (2011).
[5] ITER Physics Expert Group on Diagnostics and ITER Physics Basis Editors, Nucl. Fusion **39**, 2541 (1999).
[6] S. Tugarinov *et al.*, in *Advanced Diagnostics for Magnetic and Inertial Fusion*, edited by P. E. Stott, A. Wootton, G. Gorini, E. Sindoni, and D. Batani (Springer, Boston, MA, 2002), p. 253.
[7] S. Tugarinov *et al.*, Rev. Sci. Instrum. **74**, 2075 (2003).
[8] S. N. Tugarinov *et al.*, Plasma Phys. Rep. **30**, 128 (2004).
[9] M. von Hellermann *et al.*, Rev. Sci. Instrum. **75**, 3458 (2004).
[10] A. Malaquias *et al.*, Rev. Sci. Instrum. **75**, 3393 (2004).
[11] M. von Hellermann *et al.*, Rev. Sci. Instrum. **77**, 10F516 (2006).
[12] M. G. von Hellermann *et al.*, AIP Conf. Proc. **988**, 165 (2008).
[13] M. G. von Hellermann *et al.*, Nucl. Instrum. Methods Phys. Res., Sect. A **623**, 720 (2010).
[14] S. V. Serov, S. N. Tugarinov, and M. von Hellermann, in *45th EPS Conference* (European Physical Society, 2018), p. P4.1012; available at http://ocs.ciemat.es/EPS2018PAP/pdf/P4.1012.pdf
[15] P. Mertens, J. Fusion Energy **38**, 264 (2019).
[16] S. V. Serov, S. N. Tugarinov, and M. von Hellermann, in *3rd European Conference on Plasma Diagnostics ECPD* (Técnico Lisboa, 2019), p. P1.17; available at https://www.ipfn.tecnico.ulisboa.pt/ECPD2019/pdf/ecpd2019_book_of_abstracts.pdf
[17] M. von Hellermann *et al.*, Atoms **7**, 30 (2019).
[18] H. P. Summers, The ADAS User Manual, http://www.adas.ac.uk/.
[19] M. G. von Hellermann *et al.*, Phys. Scr. **2005**, 19.
[20] R. J. E. Jaspers *et al.*, Rev. Sci. Instrum. **79**, 10F526 (2008).
[21] J. Huang *et al.*, Rev. Sci. Instrum. **87**, 11E542 (2016).
[22] A. J. H. Donné *et al.*, Nucl. Fusion **47**, S337 (2007).
[23] L. Garzotti *et al.*, Nucl. Fusion **59**, 026006 (2018).
[24] S. N. Tugarinov *et al.*, Instrum. Exp. Tech. **59**, 104 (2016).
[25] S. Kajita, M. De Bock, M. von Hellermann, A. Kukushkin, and R. Barnsley, Plasma Phys. Controlled Fusion **57**, 045009 (2015).
[26] S. Menmuir *et al.*, Rev. Sci. Instrum. **85**, 11E412 (2014).
[27] L. A. Klyuchnikov *et al.*, Rev. Sci. Instrum. **87**, 053506 (2016).
[28] A. Kappatou *et al.*, Plasma Phys. Controlled Fusion **60**, 055006 (2018).
[29] A. Y. Shabashov, S. V. Serov, S. N. Tugarinov, and V. P. Yartsev, Instrum. Exp. Tech. **62**, 675 (2019).